

See discussions, stats, and author profiles for this publication at: <https://www.researchgate.net/publication/338071622>

Paleogene Marine and Terrestrial Development of the West Antarctic Rift System

Article in Geophysical Research Letters · December 2019

DOI: 10.1029/2019GL085281

CITATIONS

0

READS

74

6 authors, including:



Jason Coenen
Northern Illinois University

21 PUBLICATIONS 70 CITATIONS

[SEE PROFILE](#)



Reed P. Scherer
Northern Illinois University

174 PUBLICATIONS 3,172 CITATIONS

[SEE PROFILE](#)



Sophie Warny
Louisiana State University

89 PUBLICATIONS 1,072 CITATIONS

[SEE PROFILE](#)

Some of the authors of this publication are also working on these related projects:



IODP 364 [View project](#)



Southern Ocean Studies [View project](#)

Geophysical Research Letters

RESEARCH LETTER

10.1029/2019GL085281

Key Points:

- Paleogene marine and terrestrial subglacial microfossils from the West Antarctic interior provide insights into basin history and structure
- Subglacial fossils and biomarkers suggest that the regional paleotopography was significantly lower than implied by published reconstructions
- The regional differences in subglacial fossils and biomarkers further highlight a central divide that exists in the Ross Embayment

Supporting Information:

- Supporting Information S1

Correspondence to:

J. J. Coenen,
jcoenen@niu.edu

Citation:

Coenen, J. J., Scherer, R. P., Baudoin, P., Warny, S., Castañeda, I. S., & Askin, R. (2020). Paleogene marine and terrestrial development of the West Antarctic Rift System. *Geophysical Research Letters*, 47, e2019GL085281. <https://doi.org/10.1029/2019GL085281>

Received 4 SEP 2019

Accepted 9 DEC 2019

Accepted article online 19 DEC 2019

Paleogene Marine and Terrestrial Development of the West Antarctic Rift System

J. J. Coenen¹ , R. P. Scherer¹ , P. Baudoin² , S. Warny² , I. S. Castañeda³ , and R. Askin²

¹Department of Geology and Environmental Geosciences, Northern Illinois University, DeKalb, IL, USA, ²Department of Geology and Geophysics and Museum of Natural Science, Louisiana State University and A. & M. C., Baton Rouge, LA, USA, ³Department of Geosciences, University of Massachusetts Amherst, Amherst, MA, USA

Abstract Modeling the early development of the West Antarctic Ice Sheet (WAIS) hinges on the configuration and evolution of Paleogene terrestrial landscapes associated with the West Antarctic Rift System. A widely applied but previously untested paleotopographic reconstruction for the Eocene/Oligocene boundary suggests that much of central West Antarctica was as much as 1,000 m above sea level at that time, constituting a key nucleating site for an early WAIS. Here we show that Paleogene age marine and terrestrial microfossil assemblages and biomarkers in sediments recovered from beneath the WAIS provide direct evidence contrary to this widely utilized “maximum” paleotopographic reconstruction. These new constraints call for significantly modified tectonic and ice sheet model parameterization and also provide insights into modern differential uplift across the West Antarctic Rift System.

Plain Language Summary The configuration and elevation of Antarctic land masses played a key role in early ice sheet development in a world with CO₂ much higher than today's. Several studies have attempted to reconstruct the terrestrial landscape of the tectonically complex West Antarctica 34 million years ago, a time when a cooling climate led to Antarctic ice sheet growth. Here we use sedimentary records collected from beneath the West Antarctic Ice Sheet interior to test published landscape reconstructions for this critical interval in Earth history. Marine microfossils (diatoms, dinoflagellates, calcareous nannofossils, and ebridians) are used to constrain the ages of sedimentary deposits. Additionally, we use terrestrial pollen, spores, and freshwater diatoms, as well as marine and terrestrial organic biomarkers, to document past sedimentary basins and reconstruct paleoenvironments during the transition from the warm Eocene (~56 to 34 million years ago) to the cooler Oligocene (~34 to 23 million years ago). Our results significantly advance knowledge of tectonic and landscape evolution across West Antarctica, thus calling for improved modeling of the early ice sheet.

1. Introduction

West Antarctica is characterized by high heat flow and a low-viscosity mantle (Whitehouse et al., 2019) that developed prior to Cretaceous/early Paleogene initiation of the WARS. Based on thermal subsidence estimates, plate movement and glacial erosion inferred from seismically defined offshore sedimentary bodies (Paxman et al., 2019; Wilson et al., 2012, 2013), models reconstructing the Antarctic landmass suggest that extensive uplands and coastal lowlands existed in the Ross Embayment sector of West Antarctica during Late Eocene time. Evaluating Late Paleogene paleotopographic conditions is important because one of two alternate published paleolandscape models (Wilson et al., 2012) has been widely applied in paleoglaciological (Levy et al., 2016) and paleotectonic (Whitehouse et al., 2019) studies. Uncertainties associated with model input data led the authors (Wilson et al., 2012, 2013) to present two alternative reconstructions for the end of the Eocene: a “minimum” reconstruction, characterized by coastal lowlands, and a “maximum” reconstruction that includes a broad landmass with uplands reaching 1,000-m above sea level across the southern Ross Embayment (a term we will use to encompass the entire study area; Figure 1b). Ice sheet models suggest that glaciers coalesced over highlands, spreading to lowlands as the Antarctic cooled, leading to the growth of ephemeral continental scale ice sheets, including marine-based ice sheets in the Oligocene (DeConto & Pollard, 2003). The model results are highly dependent on the topographic inputs (Colleoni et al., 2018; Galeotti et al., 2016; Gasson et al., 2015, 2016; Paxman et al., 2019; Wilson et al., 2013), which have not been constrained by proximal geologic data in the Ross Embayment (Figure 1b). New geological

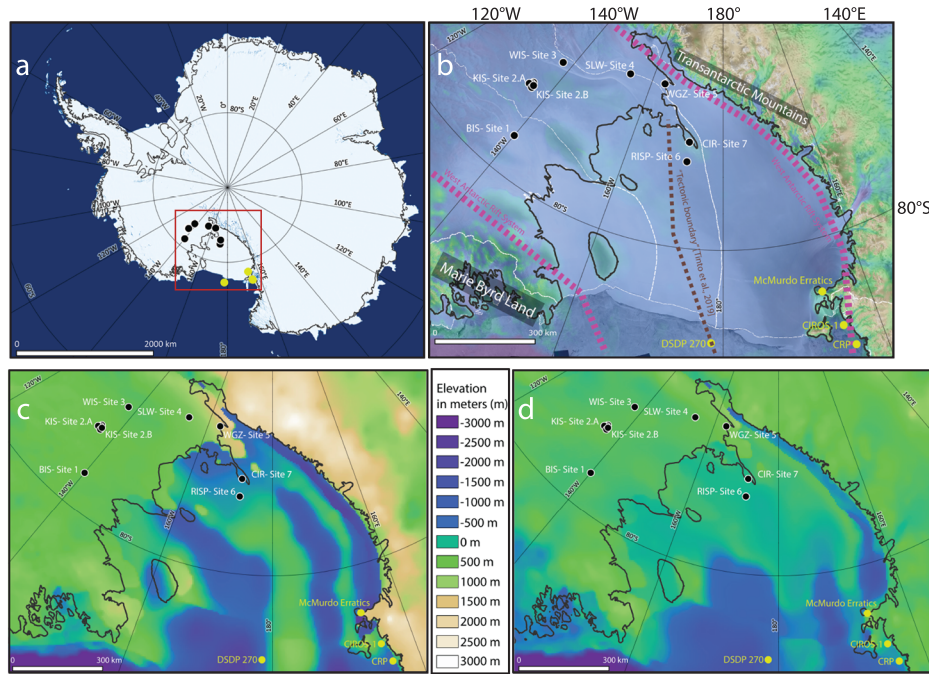


Figure 1. (a) Antarctic map highlighting sample locations (Scambos et al., 2007). (b) Sample sites highlighting the ice stream margins (Jezek et al., 2013), modern grounding line (black lines; Bindschadler et al., 2011), drainage divides (white dashed lines; Zwally et al., 2012), dashed magenta lines approximate boundaries of the West Antarctic Rift System (Bingham et al., 2012), dashed brown line marks the location of tectonic divide mapped by ROSETTA-Ice airborne geophysical data (Tinto et al., 2019), and modern basal topography (Fretwell et al., 2013). Color scale (between c and d) indicates meters above sea level of bed topography for maps (b)–(d). (c) “maximum” and (d) “minimum” reconstructions from Paxman et al. (2019) with our studied site locations on the most recent Eocene-Oligocene Paleotopography reconstructions (Text S6). For the purpose of this paper we use Ross Embayment to represent the region our sample locations cover (Figures 1b and 1c) that are labeled 1–6: (1) Bindschadler Ice Stream, (2) Kamb Ice Stream, (3) Upstream Whillans Ice Stream (**UpB** in earlier literature), (4) Subglacial Lake Whillans, downstream Whillans Ice Stream, (5) Whillans Ice Stream grounding zone, (6) Ross Ice Shelf Project (Site J-9 in earlier literature), (7) Crary Ice Rise (This figure is made using QGIS; QGIS Development Team, 2019). Also shown (yellow) are Cape Roberts Project (CRP) and Cenozoic Investigation of the Western Ross Sea core (CIROS-1), drilled sites both part of the Victoria Land Basin, DSDP Site 270, and the McMurdo Erratics locations (Harwood & Bohaty, 2000).

constraints on the paleolandscape (presented in this study) are crucial for improving paleotopographic reconstructions and, therefore, ice sheet models.

The only available direct geological evidence of WARS Paleogene basin strata is eroded and mixed subglacial sediments recovered by hot water drilling through Siple and Gould Coast ice streams. Sparse in situ Paleogene deposits are known from outcrop, drill cores and dredge samples from around Antarctica, rare Paleogene glacial erratic cobbles have been identified, and shipboard seismic studies have imaged inferred Paleogene deposits on the continental shelf such as Coulman High (e.g., De Santis et al., 1995; Escutia et al., 2019). Rare glacial sediments recovered from beneath the West Antarctic Ice Sheet (WAIS), far from any subaerially exposed landmasses, contain regionally or locally displaced and mixed microfossil and biomarker evidence of Paleogene deposition in the basin interior (Texts S1 and S2 in the supporting information). Recovered sediments (Figure 1b) are tills, eroded and mixed by glaciers (Scherer et al., 2005) during repeated growth and decay of the WAIS (Scherer, 1991). Our analyses show that these tills contain terrestrial and marine microfossils and biomarkers, which document Paleogene woodlands and coastal wetlands and also extensive neritic and pelagic marine habitats across the basin. Though stratigraphically mixed, they provide clear evidence of a range of past West Antarctic interior depositional systems, providing a direct test of inferred late Paleogene environments, and can be used to test published model-based paleotopographic reconstructions (Paxman et al., 2019; Wilson et al., 2012) (Figures 1c and 1d).

2. Materials and Methods

Sediments from 11 boreholes, drilled through the ice sheet at seven sites in the Ross Embayment (Figure 1 and supporting information Table S3.1) were analyzed for marine and terrestrial microfossils and organic

geochemistry (Text S3). These sediments were originally collected for glaciological and paleoglaciological studies (Kamb, 2001; Scherer et al., 1998). From these sediments, marine depositional events are identified from diatoms and siliceous flagellates, calcareous marine microfossils, dinoflagellate cysts, and biomarkers. The presence of isoprenoid glycerol dialkyl glycerol tetraethers (GDGTs) produced by marine Thaumarchaeota (Schouten et al., 2002; Schouten et al., 2013), in conjunction with low branched and isoprenoid tetraether (BIT) index (Hopmans et al., 2004) values, indicates marine deposits (Hopmans et al., 2004; Hopmans et al., 2016) (Texts S3 and S4 in the supporting information). Marine diatoms were documented for biostratigraphic assessment by microsieveing and counting using the Warnock and Scherer (2015) method. Palynomorphs were processed for biostratigraphic and paleoenvironmental assessment, with palynomorph concentrations calculated using the Benninghoff (1962) equation. Biomarkers in these tills build on a framework of compound distributions and aid in the establishment of paleoenvironmental interpretations utilizing approaches employed for differentiating till deposits in Hudson Bay (Battram et al., 2015) and Oligocene and Miocene sediments from the Ross Sea (Duncan et al., 2019). Here, terrestrial history is inferred from pollen and spores, plant fragments, nonmarine diatoms and chrysophyte cysts, long-chain plant leaf waxes (Eglinton & Hamilton, 1967), high BIT index values and abundant branched GDGTs (Weijers et al., 2006; Weijers et al., 2007). Age control for these deposits comes from biostratigraphic assessment of marine diatoms and other microfossils, which has been established over the last >50 years of global ocean and Antarctic drilling (Barron et al., 2015; Escutia et al., 2019) (e.g., DSDP, ODP, IODP, CRP-3, and CIROS-1; Texts S1 and S5).

3. Results: Marine Evidence

Miocene-dominated diatom assemblages were previously reported from sediment recovered from Crary Ice Rise (Site 7; Scherer et al., 1988) and from our Sites 3 (Scherer, 1991; Scherer et al., 1998) and 6 (Harwood et al., 1989), along with rare Pliocene and Pleistocene diatoms previously reported from Site 3 (Figure 1; Scherer, 1991; Scherer et al., 1998). Glacially reworked Miocene age diatoms are often common in Holocene age sediments in the Ross Sea as well, indicating glacial erosion, mixing, and transport (Sjunneskog & Scherer, 2005).

New analyses from Sites 2–5 show that Miocene, Pliocene, and Pleistocene diatoms are widespread beneath the Whillans and Kamb ice streams whereas Site 1 contains no evidence of post-Paleogene fossils (Figure 1b). Relatively rare reworked Paleogene fossils occur in all samples studied, along with long-ranging robust diatoms that are typical of, but not exclusive to, Paleogene deposits, (e.g., *Stephanopyxis*, *Stellarima*, and *Paralia* spp.). We identify biostratigraphically unique Paleogene taxa, including several well-constrained diatom, dinoflagellate, and calcareous nannofossil species from which we identify two distinct Paleogene age source beds (Figure 2a and Text S5). We define the two separate Paleogene depositional events as (1) Mid-Paleogene Marine Event (MPME) dating between ~47 and 45 Ma, which is observed in other studies of this time interval in the high southern latitudes (e.g., Barron et al., 2015; Fenner, 1984) (Figure 2a) and (2) Late-Paleogene Marine Event (LPME) constrained between ~34.5 and 31.5 Ma (Figure 2a).

LPME occurs in Sites 2–6 samples, whereas MPME is unique to Site 1, which contains no microfossils specifically attributable to Miocene and younger strata (Table S1.1). The MPME assemblage is characterized by the marine diatoms *Trinacria simulacrum*, *Stephanopyxis grunowii*, *Triceratium crenulatum*, and *Pterotheca aculeifera* as well as common *Pyxilla reticulata* (Barron et al., 2015; Fenner, 1978; Hajós, 1976). Although biomarkers are not age diagnostic, notably high GDGT-inferred temperatures at Site 1, which are well above modern mean annual air or sea surface temperatures in the region (Nicolas & Bromwich, 2014), suggest deposition under elevated warmth (Figures 3e–3g). The high abundance of terrestrial material in Site 1 relative to marine may suggest that this marine incursion was transitory (Figures 3a and 3f). The MPME likely accumulated in the West Antarctic interior coincident with widespread Eocene biosiliceous sedimentation near Antarctica's coast (Barron et al., 2015; Harwood & Bohaty, 2000; Stickley et al., 2004).

Sites 3–5 contain a pronounced LPME assemblage (Barron et al., 2015; Harwood & Bohaty, 2001; Harwood, 1989; Gombos & Ciesielski, 1983; Dzinoridze, 1978; Fenner, 1978; McCollum, 1975; Hajós, 1975) characterized by the diatoms *Pseudotriceratium radiosoreticulatum*, *Skeletonenia utriculosa*, *Hemiaulus polycystorum*, and *Pyxilla reticulata*; the ebridian *Ammodochium ampulla*; the dinoflagellate cysts *Vozzhennikovia apertura* and *Spinidinium macmurdense*; and a latest Eocene-early Oligocene *Reticulofenestra*-bearing calcareous nannofossil assemblage (Figure 3a) previously described from Site 3

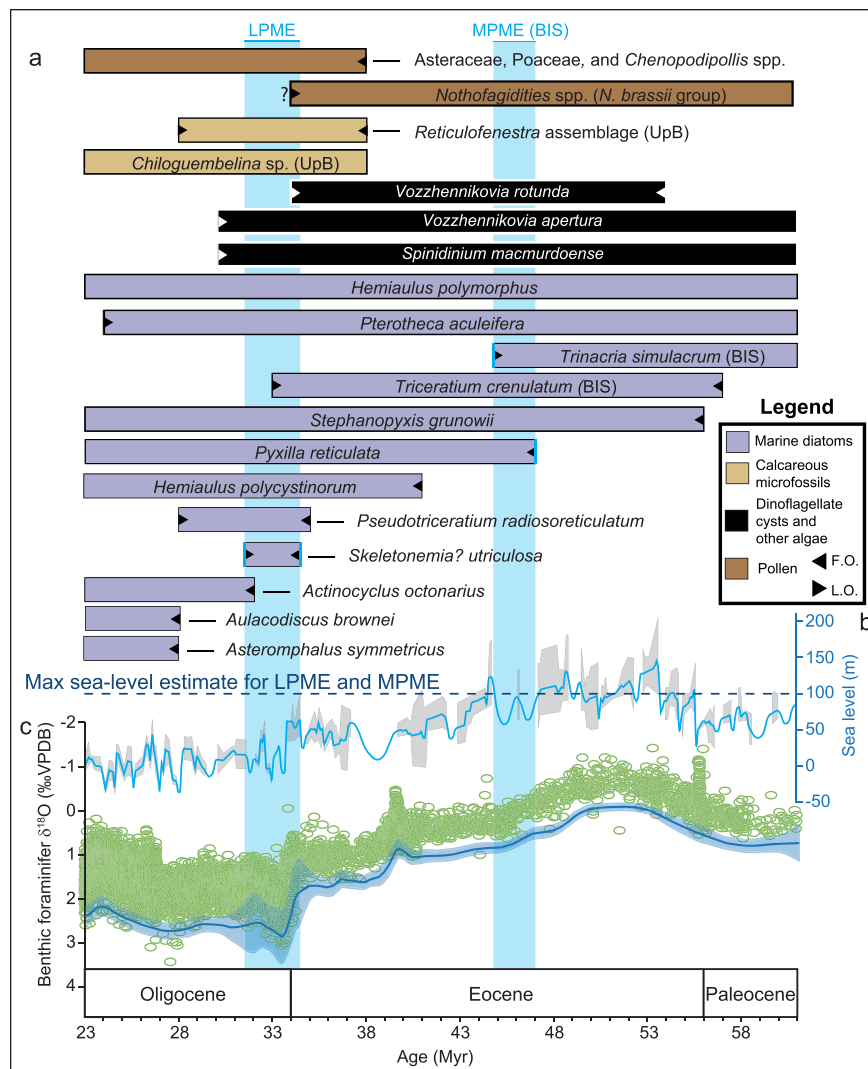


Figure 2. (a) Biostratigraphic age ranges plotted with proxy records used to infer Paleogene marine events from studied sites. Total age ranges of taxa are represented by their respective color bars (see legend) with first occurrences (F.O.) representing the earliest the taxon has been observed in the Antarctic region, and the last occurrence (L.O.) representing the youngest occurrence the taxon has been observed in Antarctic strata. These overlaps are used to define the ranges that represent inferred Late Paleogene Marine Event (LPME) and Mid-Paleogene Marine Event (MPME) indicated by blue bars. (b) A reconstruction of sea level from the New Jersey margin shows minimum uncertainty (gray envelope), best estimate (blue line; Kominz et al., 2008), and max sea level during defined Paleogene events (dashed dark blue line). (c) A composite of southern hemisphere high latitude benthic foraminifer $\delta^{18}\text{O}$ (green) is recorded with uncertainty band (blue) calculated from Mudelsee et al. (2014), reflecting global ice volume and changes in deep water temperatures. Diatoms *Actinocyclus octonarius*, *Aulacodiscus brownei*, and *Asteromphalus symmetricus* represent the oldest possible ages for Miocene assemblages (not present at Site 1, BIS).

(Scherer, 1991). A single fragmented biserial planktonic foraminifer (likely *Chiloguembelina* sp.) was also noted at Site 3 (Scherer, 1991).

4. Results: Terrestrial Evidence

Paleogene terrestrial West Antarctic interior landscapes are inferred from small freshwater diatom-rich sediment clasts with plant debris, chrysophyte cysts (Scherer, 1991) and Zygnemataceae (green algae). Site 4 sediments contain similar freshwater diatoms previously observed from Site 3 (Scherer, 1991). However, concentrations are much lower and only observed as isolated valves.

Samples from all sites contain a high diversity of southern beech pollen, *Nothofagidites* spp., with at least 12 different morphotypes (Text S7). One key group observed is *Nothofagidites* spp. of the *N. brassii* group, a morphotype that disappeared regionally as Antarctica cooled at the close of the Late Eocene (Warny et al., 2009;

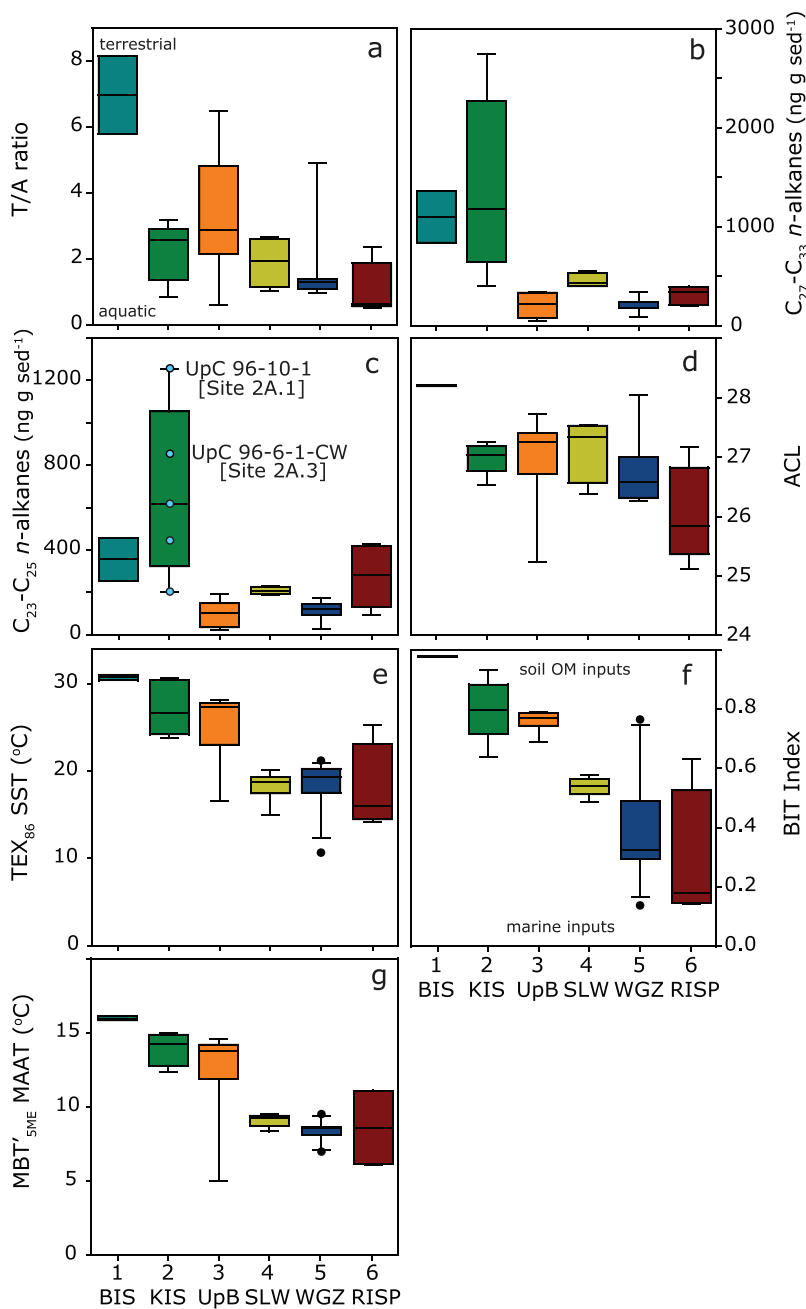


Figure 3. Box plots of biomarker data; site number are the same as in Figure 1. (a) The Terrestrial/aquatic (T/A) *n*-alkane ratio (Eglinton & Hamilton, 1967; Meyers, 1997). Site 1 (BIS) has the highest T/A value (terrestrial inputs). (b and c) Total long-chain (C_{27} - C_{33}) and middle-chain (C_{23} and C_{25}) *n*-alkane concentrations in units of ng alkanes per g sediment extracted. For the KIS sites, individual data points are indicated by the light blue circles. Two labeled samples, UpC 96-10-1 and UpC 96-6-1-CW, have elevated concentrations of middle-chain *n*-alkanes. These samples are equivalent to sample UpC-96-10-CW, which contained a rich assemblage of sphagnum spores and included visible lignite fragments. (d) *n*-alkane average chain length (Bush & McInerney, 2013). (e) TEX_{86} sea surface temperature (SST) estimates. There are multiple TEX_{86} SST calibrations (e.g., Schouten et al., 2002; Tierney & Tingley, 2014); here we apply the (Kim et al., 2008) calibration. (f) MBT'_{5ME} mean annual air temperature (MAAT) estimates (De Jonge et al., 2014). For reference, today MAAT in Antarctica ranges from ~0 °C near the coast to -50 °C in the continental interior (Nicolas & Bromwich, 2014). Notably, both TEX_{86} and MBT'_{5ME} yield similar patterns and all sites reconstructed these temperatures are well above modern temperatures, pointing to the inclusion of older material from past warm climates in the glacial tills. At Site 1 (BIS), which lacks microfossils from post Paleogene strata, the highest TEX_{86} and MBT'_{5ME} values occur, consistent with a dominantly Eocene greenhouse origin as suggested by diatom assemblages. (g) BIT Index; Site 1 (BIS) is dominated by soil inputs in agreement with (a). See the supporting information for more details on all biomarker proxies.

Warny & Askin, 2011b). Additionally, there are diverse Proteaceae, well-preserved podocarps, and other gymnosperms, including *Phyllocladidites* spp., suggesting a proximal rain forest (Figure 2a). Few spores were observed at Sites 3 and 5; however, one sample from Site 2A (Table S3.1) is unique in that in addition to the diverse assemblage of terrestrial pollen and spores, it contains a rich assemblage of *Sphagnum* (bryophyte) spores and visible lignite fragments, indicative of boggy deposits.

Two equivalent biomarker samples at Site 2 (Figure 3c) contain significantly higher concentrations of the middle-chain C₂₃ and C₂₅-n-alkanes, which are biomarkers of *Sphagnum* mosses (Nott et al., 2000) (Text S4.1). Site 1, with its exclusively Paleogene marine flora, contains notably high concentrations of well-preserved pollen and plant leaf waxes, suggesting proximity to source strata (Figures 2a and 3 and Text S4.1). Thus, in contrast to Site 2, low spore concentrations at Site 1 suggest that pteridophytes and/or bryophytes were regionally rare at the time of this deposition, which likely predated the MPME.

5. Discussion

Differences among microfossil concentrations and assemblages between sites provide insights into the regional tectonic history and relative rates of glacial isostatic rebound. Studies of West Antarctic basin evolution highlight a long history of Cenozoic deposition associated with the WARS (McKay et al., 2016; Paxman et al., 2019 ; Wilson et al., 2012). The distinct microfossil assemblages observed at Site 1, the closest ice stream to Marie Byrd Land (Figure 1b), suggests a different basin evolution than those near the Transantarctic Mountains, such as Sites 3–7 and the CIROS-1 and CRP-3 cores (Davey et al., 2006; Harwood, 1989; Harwood & Bohaty, 2001; Spiegel et al., 2016). This difference is mirrored in detrital zircon populations of the basin bordering Marie Byrd Land versus those bordering the Transantarctic Mountains (Licht et al., 2014). Evidence of emergent bedrock above sea level in the Ross Sea comes from marine seismic surveys that imaged narrow troughs, interpreted as alpine glacial valleys, cut into bedrock of the Central High (De Santis et al., 1995). Paleotopography models depict a prominent elongate range (Paxman et al., 2019; Wilson et al., 2012) (Figures 1c and 1d) that, together with a tectonic boundary revealed by the ROSETTA-Ice geophysical survey (Tinto et al., 2019), likely prevented communication between the basins.

Additionally, the Marie Byrd Land region has a higher uplift potential as a result of a thinner crust with a low viscosity, responsive mantle (Whitehouse et al., 2019) likely influenced by an inferred mantle plume (Winberry & Anandakrishnan, 2004; Begeman et al., 2017; Nield et al., 2018; Barletta et al., 2018; Fisher et al., 2015). Spiegel et al. (2016) suggest the uplift arising from plume activity occurred ~20 Ma. These mechanisms might contribute to differential uplift or subsidence across the Ross Embayment, contributing to the regional differences observed in the subglacial sediments.

Marine deposits accumulated across the broad basin during times lacking grounded ice or ice shelves, but subsequent glacial activity led to significant erosion and transport of these deposits (Paxman et al., 2019; Wilson et al., 2012). Reworked Upper and Middle Miocene diatoms occur at Site 6 (Harwood et al., 1989), but Lower Miocene diatoms dominate, including abundant soft sediment clasts of Lower Miocene diatomite, suggesting that in situ Lower Miocene strata unconformably lie beneath the glacial sediments at the seafloor (Harwood et al., 1989). The strong dominance of Upper Miocene diatoms beneath Sites 2–5, and Site 7 (Scherer et al., 1998), suggests a regional age of currently eroding strata beneath the till. Site 1, lacking younger microfossils, indicates active erosion of Eocene strata, which is supported by notably high reconstructed GDGT temperatures (Figures 3e and 3g and Text S4). Additionally, Site 1 has an average chain length of 28.2 (Figure 3d), which is consistent with Eocene age erratic boulders in the McMurdo Sound region (Duncan et al., 2019). Currently, Whillans and Bindschadler ice streams are of similar thickness and flow rates (Kamb, 2001). Consequently, basal erosion rates as well as till deformation and downstream sediment transport processes should be comparable. The absence of Neogene fossils at Site 1 therefore implies deeper glacial erosion than at the other sites, with ongoing unroofing and removal of younger strata. Because Miocene and younger marine strata must have accumulated there during periods of reduced ice, the lack of young fossils implies significantly more uplift at Site 1 than the others; a conclusion consistent with tectonic interpretations (Whitehouse et al., 2019; Winberry & Anandakrishnan, 2004; Begeman et al., 2017; Nield et al., 2018; Barletta et al., 2018; Fisher et al., 2015; Spiegel et al., 2016).

Terrestrial evidence is inferred from diatomaceous clasts in sediments from beneath the upstream part of Whillans Ice Stream (Site 3), which represents lowland lake deposits that likely existed further south

(Scherer, 1991). Although these freshwater diatomites cannot be directly dated, we infer that they predate LPME flooding/subsidence associated with rifting. These freshwater diatoms also occur in trace amounts at Site 4 (Subglacial Lake Whillans), 220 km directly downstream of Site 3, indicating subglacial transport (Text S2). Northward dilution of the terrestrial components beneath the ice stream is supported by the BIT index trend from Site 3 to Site 4 (Figure 3f).

Our terrestrial observations are consistent with previous palynological studies, which reveal that as the Antarctic climate cooled from the Eocene to the Miocene (Figure 3c), diverse angiosperms and gymnosperms were progressively replaced by a largely monospecific assemblage of *Nothofagidites*, with rare conifers, and more abundant bryophytes. Pollen and spores consistent with Miocene tundra assemblages are common in Miocene age Ross Sea sediment (Warny et al., 2009; Warny & Askin, 2011b).

Terrestrial palynomorph concentrations in subglacial samples (Text S7) reach up to almost 4 times higher than the highest concentration (60,000 p/gds) in situ latest Eocene pollen and spores in the SHALDRIL section (Warny & Askin, 2011b), implying proximity to source beds. To further place our concentration values into a larger context, younger in situ sections also sampled during the SHALDRIL II campaign (Warny & Askin, 2011a), yielded concentrations below 1,000 p/gds for the Oligocene, to concentrations up to 10,000 p/gds in mid-Miocene samples. Again, we cannot compare yields from in situ sections to yields from tills, though the very high concentration values found in the subglacial tills are likely indicative of a Late Eocene age. The *Nothofagidites* (southern beech) pollen are extremely well preserved. Preservation, very high concentrations, and most of all, the presence of clusters (Warny & Askin, 2011a), all can be seen as evidence that the vegetation source was close to the deposition sites.

The marine basin history likely started with extension in the Site 1 region with subsidence leading to marine flooding of terrestrial environments and the subsequent accumulation of marine fossils during Early to Middle Eocene intervals. Upper Eocene through Lower Oligocene marine strata were more widespread across West Antarctica, as evidenced by widely distributed microfossils, including diverse marine environments characterized by calcareous nannofossils, diatoms, ebridians, planktic foraminifera, and dinoflagellate cysts (Figure 3a). The marine diatoms that make up the LPME are comparable to the assemblage defined as Association Zone B from Harwood (1989) at CIROS-1 (Figures 1b–1d). Furthermore, diatom assemblages identified in the Cape Roberts Project Core CRP-3, part of the Victoria Land Basin (Harwood & Bohaty, 2001) were used define the total age ranges used for our estimates of the LPME. Most notably Site 5 has an assemblage that fits with an Early Oligocene assemblage defined by CIROS-1 and CRP-3 studies, further supporting a widespread depositional event during this interval.

Pollen, spores (including abundant *Sphagnum* at Site 2), plant fragments, nonmarine diatoms, and terrestrial leaf waxes indicate extensive Paleogene coastal lowland environments and forests across the WARS over terrains now well below sea level (Figures 1b–1d). DSDP Site 270, used to define paleotopography models for the early Oligocene, has evidence of pre-Late Oligocene terrestrial paleosols that indicate terrestrial conditions at circa 34 Ma (Ford & Barrett, 1975). Recently, chronostratigraphy of Site 270 was refined by K-Ar dating of the glauconitic greensand that overlies terrestrial paleosols (Kulhanek et al., 2019). The glauconite dated to 26–25 Ma, and paleoenvironmental evidence from this interval infers a shallow marine setting during the late Oligocene that deepened through subsidence into the Miocene (Figures 1b–1d) (Kulhanek et al., 2019). Site 270 has been used as a proximal constraint in Paxman et al. (2019) models, which does fit with the paleoenvironments described; however, our study sites indicate some deeper marine settings that extend into the interior (Figures 1c, 1d, and 2a), requiring Site Locations 2–5 to be much lower than is suggested by paleotopographic models (Paxman et al., 2019; Wilson et al., 2012, 2013).

Rifting initially occurred over subaerially exposed landscapes, developing lakes and coastal lowlands including *Sphagnum* bogs prior to the development of a large ice sheet. The last phase of this rifting event is particularly prominent at Site 5, where abundant ebridians, sea ice indicating acritarchs (*Leiosphaeridia*), and the diatoms *P. radiosoreticulatum* and *Pyxilla reticulata* represent Late Oligocene to Early Miocene neritic marine conditions with the expansion of seasonal sea ice as Antarctica cooled. Paleotopographic models from Wilson et al. (2012, 2013) and more recently Paxman et al. (2019) provide critical boundary conditions for ice sheet and climate modeling for the Paleogene onset and early Neogene variability of major glaciation in West Antarctica (Galeotti et al., 2016; Gasson et al., 2016; Levy et al., 2016; McKay et al., 2016; Paxman et al., 2019). However, the large uncertainty regarding these models in the Ross Embayment has led to

the presentation of two alternative reconstructions: “maximum” and “minimum.” Only the maximum reconstruction has been utilized as boundary conditions for studies, until Pollard and DeConto (2019) recently used a simple average of “maximum” and “minimum” (Wilson et al., 2012) and Paxman et al. (2019) made an updated model. Yet our results indicate that the basin inferred by paleotopography models (Paxman et al., 2019; Wilson et al., 2012, 2013) was locally below sea level during the LPME (34.5–31.5 Ma) and MPME (47–45 Ma), providing direct evidence of depositional paleoenvironments broadly consistent with their minimum reconstructions (Text S6), especially when global sea level estimates are considered (Figure 2b).

Lacking better sample site coverage, it is not possible to know with certainty how far these microfossils have been glacially transported. However, the abundance and good preservation of the marine fossils give strong indications that the material is derived from nearby eroding source beds (see Scherer et al., 2005; Sjunneskog & Scherer, 2005 for discussion). Given our knowledge of the regional topography, the tectonic history of the basin, and ice sheet basal processes, material would have been transported a relatively short distance from upstream by subglacial or englacial processes.

Due to the modern configuration (Figure 1b) of ice streams, we propose Sites 1–3 were likely in “graben blocks” that modern ice streams are currently filling, whereas current features such as Siple Dome and Engelhardt Interstream Ridge likely define “horst block” highlands. The distribution of fossils in the “graben blocks” suggests that modern ice stream troughs would have been Eocene/Oligocene marine embayments at least. Only with samples from the “horsts” could we establish the full marine extent. With these constraints we chose a conservative interpretation of marine extent during the marine events.

These observations may cast doubt on modeled extent of WAIS growth at circa 34 Ma, as the high topographies suggested in the maximum reconstructions likely did not exist (Paxman et al., 2019; Wilson et al., 2013) (Figures 1c, 1d, 2b, and 2c).

6. Conclusions

Updated ice sheet and tectonic reconstructions should utilize parameters established by analysis of subglacial sediments because they provide a wealth of proximal paleoenvironmental information about the Cenozoic development of the West Antarctic basin. Our data provide clear biostratigraphic and paleoenvironmental evidence favoring the “minimum” paleotopographic reconstruction hypotheses (Paxman et al., 2019; Wilson et al., 2012), indicating more extensive marine incursion than the “maximum” reconstructions, which are dominated by subaerial exposure with elevations up to 1,000 m at the Eocene-Oligocene transition. Basin history, including the recognition of deeper glacial erosion into older strata, can be inferred by differences in microfossil assemblages observed in till overlying eroding strata. Despite the scarcity of materials available, paleoenvironmental evidence and inferred tectonic history obtained from this study can be used to interpret key elements of Paleogene basin development in the WARS, thus better constraining deep-time ice sheet and tectonic modeling of West Antarctica. Further, the study highlights the value of and need for additional subglacial sediment recovery from beneath the Antarctic Ice Sheet.

References

- Barletta, V. R., Bevis, M., Smith, B. E., Wilson, T., Brown, A., Bordoni, A., et al. (2018). Observed rapid bedrock uplift in Amundsen Sea Embayment promotes ice-sheet stability. *Science*, 360(6395), 1335–1339. <https://doi.org/10.1126/science.aoa1447>
- Barron, J. A., Stickley, C. E., & Bukry, D. (2015). Paleoceanographic, and paleoclimatic constraints on the global Eocene diatom and silicoflagellate record. *Palaeogeography, Palaeoclimatology, Palaeoecology*, 422, 85–100.
- Battram, N. M., Eyles, N., Lau, P. S., & Simpson, M. J. (2015). Organic matter biomarker analysis as a potential chemostratigraphic tool for Late Pleistocene tills from the Hudson Bay Lowlands, Canada. *Palaeogeography, Palaeoclimatology, Palaeoecology*, 418, 377–385.
- Begeman, C. B., Tulaczek, S. M., & Fisher, A. T. (2017). Spatially variable geothermal heat flux in West Antarctica: Evidence and implications. *Geophysical Research Letters*, 44(19), 9823–9832.
- Benninghoff, W.S., 1962. Calculation of pollen and spore density in sediments by addition of exotic pollen in known quantities.
- Bindschadler, R., Choi, H., & Collaborators, A. S. A. I. D. (2011). *High-resolution Image-derived Grounding and Hydrostatic Lines for the Antarctic Ice Sheet*. Boulder, Colorado, USA: National Snow and Ice Data Center. Digital media.
- Bingham, R. G., Ferraccioli, F., King, E. C., Larter, R. D., Pritchard, H. D., Smith, A. M., & Vaughan, D. G. (2012). Inland thinning of West Antarctic Ice Sheet steered along subglacial rifts. *Nature*, 487(7408), 468–471. <https://doi.org/10.1038/nature11292>
- Bush, R. T., & McInerney, F. A. (2013). Leaf wax n-alkane distributions in and across modern plants: Implications for paleoecology and chemotaxonomy. *Geochimica et Cosmochimica Acta*, 117, 161–179.
- Colleoni, F., De Santis, L., Siddoway, C. S., Bergamasco, A., Golledge, N. R., Lohmann, G., et al. (2018). Spatio-temporal variability of processes across Antarctic ice-bed-ocean interfaces. *Nature Communications*, 9(1), 2289.

Acknowledgments

SLW and WGZ samples were recovered and analyzed as part of the WISSARD Project under NSF Awards ANT-0839107 and ANT-0839142. We thank the WISSARD team, especially R. Powell and S. Tulaczek and their students for field assistance in sediment recovery. We also thank University of Nebraska-Lincoln for hot water drill operations and the Antarctic Support Contract (ASC) for extensive field support. H. Engelhardt and the late B. Kamb are acknowledged for recovering samples from UpB, KIS, and BIS as part of their past NSF-funded West Antarctic drilling programs and thank S. Tulaczek for making some of these samples available for study. RISP cores were recovered by NSF awards to P. Webb and curated by the Antarctic Sediment Core facility at Florida State University. Funding for palynological work was provided through the NSF CAREER program (Grant 1048343 to S. W.) and through a Louisiana State University Museum of Natural Science curatorial assistantship to P. B. Funding for the biomarker analyses were partially provided by startup funds to I. S. C. at UMass. J. Wei is thanked for his work running the initial round of biomarker samples at UMass, and J. Salacup is thanked for laboratory assistance. D. Watkins, G. Villa, and D. Kulhanek are thanked for their aid in reexamining the calcareous nannofossil assemblage from UpB. J. Mastro and E. Amer Alyasiri are thanked for their help with GIS and mapping questions. C. Siddoway is thanked for edits and discussions that greatly improved this document. We would also like to thank the editor and anonymous reviewers for their insightful comments, which greatly improved the manuscript. Data supporting the conclusions of this paper will be made available through the U.S. Antarctic Program Data Center (<http://www.usap-dc.org/view/project/p0000105>).

- Davey, F. J., Cande, S. C., & Stock, J. M. (2006). Extension in the western Ross Sea region-links between Adare Basin and Victoria Land Basin. *Geophysical Research Letters*, 33(20).
- De Jonge, C., Hopmans, E. C., Zell, C. I., Kim, J. H., Schouten, S., & Damsté, J. S. S. (2014). Occurrence and abundance of 6-methyl branched glycerol dialkyl glycerol tetraethers in soils: Implications for palaeoclimate reconstruction. *Geochimica et Cosmochimica Acta*, 141, 97–112.
- De Santis, L., Anderson, J. B., Brancolini, G., & Zayatz, I. (1995). Seismic record of late Oligocene through Miocene glaciation on the central and eastern continental shelf of the Ross Sea. *Geology and Seismic Stratigraphy of the Antarctic Margin*, 68, 235–260.
- DeConto, R. M., & Pollard, D. (2003). A coupled climate–ice sheet modeling approach to the early Cenozoic history of the Antarctic ice sheet. *Palaeogeography, Palaeoclimatology, Palaeoecology*, 198(1–2), 39–52.
- Duncan, B., McKay, R., Bendle, J., Naish, T., Inglis, G. N., Mooszen, H., et al. (2019). Lipid biomarker distributions in Oligocene and Miocene sediments from the Ross Sea region, Antarctica: Implications for use of biomarker proxies in glacially-influenced settings. *Palaeogeography, Palaeoclimatology, Palaeoecology*, 516, 71–89.
- Dzinoridze, R. N. (1978). Diatom and radiolarian Cenozoic stratigraphy, Norwegian Basin; DSDP Leg 38. *Initial Reports of the Deep Sea Drilling Project*, 38, 289–385.
- Eglinton, G., & Hamilton, R. J. (1967). Leaf epicuticular waxes. *Science*, 156(3780), 1322–1335. <https://doi.org/10.1126/science.156.3780.1322>
- Escutia, C., DeConto, R. M., Dunbar, R., Santis, L. D., Shevenell, A., & Naish, T. (2019). Keeping an eye on Antarctic ice sheet stability. *Oceanography*, 32(1), 32–46.
- Fenner, J. (1978). Cenozoic diatom biostratigraphy of the equatorial and southern Atlantic Ocean. In Supko, P.R., Perch-Nielsen, K., et al., *Init. Repts. DSDP*, 39 (Suppl., Pt. 2): Washington (U.S. Govt. Printing Office), 491–624.
- Fenner, J. (1984). Eocene-Oligocene planktic diatom stratigraphy in the low latitudes and the high southern latitudes. *Micropaleontology*, 31, 319–342.
- Fisher, A. T., Mankoff, K. D., Tulaczyk, S. M., Tyler, S. W., & Foley, N. (2015). High geothermal heat flux measured below the West Antarctic Ice Sheet. *Science Advances*, 1(6), e1500093.
- Ford, A. B., & Barrett, P. J. (1975). Basement rocks of the south-central Ross Sea, Site 270, DSDP Leg 28. *Initial Reports of the Deep Sea Drilling Project*, 28, 861–868.
- Fretwell, P., Pritchard, H.D., Vaughan, D.G., Bamber, J.L., Barrand, N.E., Bell, R., et al., 2013. Bedmap2: Improved ice bed, surface and thickness datasets for Antarctica.
- Galeotti, S., DeConto, R., Naish, T., Stocchi, P., Florindo, F., Pagani, M., et al. (2016). Antarctic Ice Sheet variability across the Eocene–Oligocene boundary climate transition. *Science*, 352(6281), 76–80.
- Gasson, E., DeConto, R., & Pollard, D. (2015). Antarctic bedrock topography uncertainty and ice sheet stability. *Geophysical Research Letters*, 42(13), 5372–5377.
- Gasson, E., DeConto, R. M., Pollard, D., & Levy, R. H. (2016). Dynamic Antarctic ice sheet during the early to mid-Miocene. *Proceedings of the National Academy of Sciences*, 113(13), 3459–3464.
- Gombos, A. M. Jr., & Ciesielski, P. F. (1983). Late Eocene to Early Miocene diatoms from the Southwest Atlantic. In W. J. Ludwig et al. (Eds.), *Initial Reports of the Deep Sea Drilling Project*, 71 (Pt. 2) (pp. 538–634). Washington, DC: U.S. Government Printing Office.
- Hajós, M. (1975). Late Cretaceous Archaeomonadaceae, Diatomaceae and Silicoflagellatae from the South Pacific Ocean. Deep Sea Drilling Project Leg 29, site 275. *Initial Reports of the Deep Sea Drilling Project*, 29, 913–1109.
- Hajós, M. (1976). Upper Eocene and lower Oligocene diatomaceae, archaeomonadaceae, and silicoflagellatae in southwestern Pacific sediments, DSDP Leg 29. *Initial Reports of the Deep Sea Drilling Project*, 35, 817–883.
- Harwood, D. M. (1989). Siliceous microfossils. Antarctic Cenozoic history from the CIROS-1 drillhole, McMurdo Sound. *DSIR Bulletin*, 245, 67–97.
- Harwood, D. M., & Bohaty, S. M. (2000). Marine diatom assemblages from Eocene and younger erratics, McMurdo Sound, Antarctica. *Paleobiology and Paleoenvironments of Eocene Rocks: McMurdo Sound, East Antarctica*, 76, 73–98.
- Harwood, D. M., & Bohaty, S. M. (2001). Early Oligocene siliceous microfossil biostratigraphy of Cape Roberts Project core CRP-3. Antarctica: Victoria Land Basin.
- Harwood, D. M., Scherer, R. P., & Webb, P. N. (1989). Multiple Miocene marine productivity events in West Antarctica as recorded in Upper Miocene sediments beneath the Ross Ice Shelf (Site J-9). *Marine Micropaleontology*, 15(1–2), 91–115.
- Hopmans, E. C., Schouten, S., & Damsté, J. S. S. (2016). The effect of improved chromatography on GDGT-based palaeoproxies. *Organic Geochemistry*, 93, 1–6.
- Hopmans, E. C., Weijers, J. W., Schefuß, E., Herfort, L., Damsté, J. S. S., & Schouten, S. (2004). A novel proxy for terrestrial organic matter in sediments based on branched and isoprenoid tetraether lipids. *Earth and Planetary Science Letters*, 224(1–2), 107–116.
- Jezek, K. C., J. C. Curlander, F. Carsey, C. Wales, and R. G. Barry. 2013. RAMP AMM-1 SAR Image Mosaic of Antarctica. Boulder, Colorado USA. <https://doi.org/10.5067/8af4zrpuls4h> NSIDC: National Snow and Ice Data Center.
- Kamb, B. (2001). Basal zone of the West Antarctic ice streams and its role in lubrication of their rapid motion. *The West Antarctic ice sheet: Behavior and environment*, 77, 157–199.
- Kim, J. H., Schouten, S., Hopmans, E. C., Donner, B., & Damsté, J. S. S. (2008). Global sediment core-top calibration of the TEX86 paleothermometer in the ocean. *Geochimica et Cosmochimica Acta*, 72(4), 1154–1173.
- Kominz, M. A., Browning, J. V., Miller, K. G., Sugarman, P. J., Mizintseva, S., & Scotese, C. R. (2008). Late Cretaceous to Miocene sea-level estimates from the New Jersey and Delaware coastal plain coreholes: An error analysis. *Basin Research*, 20(2), 211–226.
- Kulhanek, D. K., Levy, R. H., Clowes, C. D., Prebble, J. G., Rodelli, D., Jovane, L., et al. (2019). Revised chronostratigraphy of DSDP Site 270 and late Oligocene to early Miocene paleoecology of the Ross Sea sector of Antarctica. *Global and Planetary Change*, 178, 46–64.
- Levy, R., Harwood, D., Florindo, F., Sangiorgi, F., Tripati, R., Von Eynatten, H., et al. (2016). Antarctic ice sheet sensitivity to atmospheric CO₂ variations in the early to mid-Miocene. *Proceedings of the National Academy of Sciences*, 113(13), 3453–3458.
- Licht, K. J., Hennessy, A. J., & Welke, B. M. (2014). The U-Pb detrital zircon signature of West Antarctic ice stream tills in the Ross embayment, with implications for Last Glacial Maximum ice flow reconstructions. *Antarctic Science*, 26(6), 687–697.
- McCollum, D. W. (1975). Diatom stratigraphy of the Southern Ocean. *Initial Reports of the Deep Sea Drilling Project*, 28, 515–571.
- McKay, R. M., Barrett, P. J., Levy, R. S., Naish, T. R., Golledge, N. R., & Pyne, A. (2016). Antarctic Cenozoic climate history from sedimentary records: ANDRILL and beyond. *Philosophical Transactions of the Royal Society A: Mathematical, Physical and Engineering Sciences*, 374(2059), 20140301.
- Meyers, P. A. (1997). Organic geochemical proxies of paleoceanographic, paleolimnologic, and paleoclimatic processes. *Organic Geochemistry*, 27(5–6), 213–250.

- Mudelsee, M., Bickert, T., Lear, C. H., & Lohmann, G. (2014). Cenozoic climate changes: A review based on time series analysis of marine benthic $\delta^{18}\text{O}$ records. *Reviews of Geophysics*, 52(3), 333–374.
- Nicolas, J. P., & Bromwich, D. H. (2014). New reconstruction of Antarctic near-surface temperatures: Multidecadal trends and reliability of global reanalyses. *Journal of Climate*, 27(21), 8070–8093.
- Nield, G. A., Whitehouse, P. L., van der Wal, W., Blank, B., O'Donnell, J. P., & Stuart, G. W. (2018). The impact of lateral variations in lithospheric thickness on glacial isostatic adjustment in West Antarctica. *Geophysical Journal International*, 214(2), 811–824.
- Nott, C. J., Xie, S., Avsejs, L. A., Maddy, D., Chambers, F. M., & Evershed, R. P. (2000). *n*-Alkane distributions in ombrotrophic mires as indicators of vegetation change related to climatic variation. *Organic Geochemistry*, 31, 231–235.
- Paxman, G. J., Jamieson, S. S., Hochmuth, K., Gohl, K., Bentley, M. J., Leitchenkov, G., & Ferraccioli, F. (2019). Reconstructions of Antarctic topography since the Eocene–Oligocene boundary. *Palaeogeography, Palaeoclimatology, Palaeoecology*, 535, 109346.
- Pollard, D., & DeConto, R. M., 2019. Continuous simulations over the last 40 million years with a coupled Antarctic ice sheet–sediment model. *Palaeogeography, Palaeoclimatology, Palaeoecology*, p.109374.
- QGIS Development Team (2019). QGIS Geographic Information System. Open Source Geospatial Foundation Project. <http://qgis.osgeo.org>
- Scambos, T., Haran, T., Fahnestock, M., Painter, T., & Bohlander, J. (2007). MODIS-based Mosaic of Antarctica (MOA) data sets: Continent-wide surface morphology and snow grain size, Remote Sensing of Environment. 111. 242–257. *Remote Sensing of Environment*, 111(2007), 242–257. <https://doi.org/10.1016/j.rse.2006.12.020>
- Scherer, R. P. (1991). Quaternary and Tertiary microfossils from beneath Ice Stream B: Evidence for a dynamic West Antarctic ice sheet history. *Global and Planetary Change*, 4(4), 395–412.
- Scherer, R. P., Aldahan, A., Tulaczyk, S., Possnert, G., Engelhardt, H., & Kamb, B. (1998). Pleistocene collapse of the West Antarctic ice sheet. *Science*, 281(5373), 82–85. <https://doi.org/10.1126/science.281.5373.82>
- Scherer, R. P., Harwood, D. M., Ishman, S. E., & Webb, P. N. (1988). Micropaleontological analysis of sediments from the Crary Ice Rise, Ross Ice Shelf. *Antarctic JUS*, 23, 34–36.
- Scherer, R. P., Sjunneskog, C. M., Iverson, N. R., & Hooyer, T. S. (2005). Frustules to fragments, diatoms to dust: How degradation of microfossil shape and microstructures can teach us how ice sheets work. *Journal of Nanoscience and Nanotechnology*, 5(1), 96–99. <https://doi.org/10.1166/jnn.2005.016>
- Schouten, S., Hopmans, E. C., & Damste, J. S. S. (2013). The organic geochemistry of glycerol dialkyl glycerol tetraether lipids: A review. *Organic Geochemistry*, 54, 19–61.
- Schouten, S., Hopmans, E. C., Schefuß, E., & Damste, J. S. S. (2002). Distributional variations in marine crenarchaeotal membrane lipids: A new tool for reconstructing ancient sea water temperatures? *Earth and Planetary Science Letters*, 204(1–2), 265–274.
- Sjunneskog, C., & Scherer, R. P. (2005). Mixed diatom assemblages in glacigenic sediment from the central Ross Sea, Antarctica. *Palaeogeography, Palaeoclimatology, Palaeoecology*, 218(3–4), 287–300.
- Spiegel, C., Lindow, J., Kamp, P. J. J., Meisel, O., Mukasa, S., Lisker, F., et al. (2016). Tectonomorphic evolution of Marie Byrd Land—Implications for Cenozoic rifting activity and onset of West Antarctic glaciation. *Global and Planetary Change*, 145, 98–115. <https://doi.org/10.1016/j.gloplacha.2016.08.013>
- Stickley, C.E., Brinkhuis, H., McGonigal, K.L., Chaproniere, G.C.H., Fuller, M., Kelly, D.C., et al., 2004. Late Cretaceous–Quaternary biomagnetostriatigraphy of ODP Sites 1168, 1170, 1171, and 1172, Tasmanian Gateway. In *Proceedings of the Ocean Drilling Program, Scientific Results* (Vol. 189, pp. 1–57). Ocean Drilling Program, College Station TX.
- Tierney, J. E., & Tingley, M. P. (2014). A Bayesian, spatially-varying calibration model for the TEX86 proxy. *Geochimica et Cosmochimica Acta*, 127, 83–106.
- Tinto, K. J., Padman, L., Siddoway, C. S., Springer, S. R., Fricker, H. A., Das, I., et al. (2019). Ross Ice Shelf response to climate driven by the tectonic imprint on seafloor bathymetry, (p. 1). *Nature Geoscience*.
- Warnock, J. P., & Scherer, R. P. (2015). A revised method for determining the absolute abundance of diatoms. *Journal of Paleolimnology*, 53(1), 157–163.
- Warny, S., & Askin, R. (2011a). Last remnants of Cenozoic vegetation and organic-walled phytoplankton in the Antarctic Peninsula's icehouse world. In *tectonic, climatic, and cryospheric evolution of the Antarctic peninsula*, (Vol. 63, pp. 167–192). Washington, DC: American Geophysical Union.
- Warny, S., & Askin, R. (2011b). Vegetation and organic-walled phytoplankton at the end of the Antarctic greenhouse world: Latest Eocene cooling events. In *tectonic, climatic, and cryospheric evolution of the Antarctic peninsula*, (Vol. 63, pp. 193–210). Washington, DC: American Geophysical Union.
- Warny, S., Askin, R. A., Hannah, M. J., Mohr, B. A., Raine, J. I., Harwood, D. M., et al. (2009). Palynomorphs from a sediment core reveal a sudden remarkably warm Antarctica during the middle Miocene. *Geology*, 37(10), 955–958.
- Weijers, J. W., Schouten, S., Spaargaren, O. C., & Damsté, J. S. S. (2006). Occurrence and distribution of tetraether membrane lipids in soils: Implications for the use of the TEX86 proxy and the BIT index. *Organic Geochemistry*, 37(12), 1680–1693.
- Weijers, J. W., Schouten, S., van den Donker, J. C., Hopmans, E. C., & Damsté, J. S. S. (2007). Environmental controls on bacterial tetraether membrane lipid distribution in soils. *Geochimica et Cosmochimica Acta*, 71(3), 703–713.
- Whitehouse, P. L., Gomez, N., King, M. A., & Wiens, D. A. (2019). Solid Earth change and the evolution of the Antarctic Ice Sheet. *Nature Communications*, 10(1), 503.
- Wilson, D. S., Jamieson, S. S., Barrett, P. J., Leitchenkov, G., Gohl, K., & Larner, R. D. (2012). Antarctic topography at the Eocene–Oligocene boundary. *Palaeogeography, Palaeoclimatology, Palaeoecology*, 335, 24–34.
- Wilson, D. S., Pollard, D., DeConto, R. M., Jamieson, S. S., & Luyendyk, B. P. (2013). Initiation of the West Antarctic Ice Sheet and estimates of total Antarctic ice volume in the earliest Oligocene. *Geophysical Research Letters*, 40(16), 4305–4309.
- Winberry, J. P., & Anandakrishnan, S. (2004). Crustal structure of the West Antarctic rift system and Marie Byrd Land hotspot. *Geology*, 32(11), 977–980.
- Zwally, H. J., Giovinetto, M. B., Beckley, M. A., & Saba, J. L. (2012). Antarctic and Greenland drainage systems, GSFC Cryospheric Sciences Laboratory, at http://icesat4.gsfc.nasa.gov/cryo_data/ant_grn_drainage_systems.php